A Novel Low-Density Lipoprotein Receptor-Related Protein Mediating Cellular Uptake of Apolipoprotein E-Enriched β-VLDL in Vitro[†,‡]

Takuya Sugiyama,[§,||] Hidetoshi Kumagai,[§,⊥] Yoshihiro Morikawa,[#] Yoichiro Wada,[▽] Akira Sugiyama,[▽] Kazuki Yasuda,[▼] Norihide Yokoi,[▼] Shinobu Tamura,[#] Tetsuo Kojima,[§] Tetsuya Nosaka,[§] Emiko Senba,[#] Satoshi Kimura,[||] Takashi Kadowaki,[||] Tatsuhiko Kodama,[▽] and Toshio Kitamura*[,§]

Department of Hematopoietic Factors, The Institute of Medical Science, University of Tokyo, Tokyo 108-8639, Japan, Department of Metabolic Diseases, Graduate School of Medicine, University of Tokyo, Tokyo 113-8655, Japan, Department of Molecular Biology and Medicine, Research Center for Advanced Science and Technology, University of Tokyo, Tokyo 153-8904, Japan, Department of Anatomy and Neurobiology, Wakayama Medical School, Wakayama 641-8509, Japan, Department of Medical Genetics, Graduate School of Medicine, Chiba University, Chiba 260-8670, Japan, and Takada Research Labs, Chugai Pharmaceutical Company, Ltd., Tokyo 171-8545, Japan

Received July 7, 2000; Revised Manuscript Received September 27, 2000

ABSTRACT: We report here the identification of a novel member of the low-density lipoprotein receptor (the LDL receptor) family through signal sequence trap screening of a mouse lymphocyte cDNA library. The protein was termed LDL receptor-related protein 9 (LRP9). LRP9 is a type I membrane protein predicted to contain 696 amino acids with a calculated molecular mass of 74 764 Da. The NH_2-terminal half of LRP9 contains two CUB domains separated by a single ligand-binding repeat. The second CUB domain is followed by a cluster of three additional ligand-binding repeats and a transmembrane domain. The COOH-terminal intracellular region contains a proline-rich region. LRP9 mRNA was expressed in the liver, kidney, lung, and heart at high levels, and in the spleen and brain at low levels. In situ hybridization analysis of mouse liver, kidney, and brain detected LRP9 transcripts in hepatocytes, sinusoidal lining cells, peritubular capillaries, choroid plexus, ependyma of the third ventricle, pia matter, and hippocampus. In particular, high levels of expression were observed in the vascular walls. Apolipoprotein E (apoE)-enriched β-VLDL stimulated cellular cholesteryl ester formation in ldl-A7/LRP9. These results raise the possibility that this newly identified receptor, which is expressed in the liver, may play a physiological role in the uptake of apoE-containing lipoproteins.

Cells can take up lipophilic molecules through several mechanisms which include simple diffusion, phagocytosis, or via specific cell surface receptors/transporters. The most extensively studied among such receptors are the low-density lipoprotein (LDL)[1] receptor and its family proteins. This family includes the LDL receptor (LDLR) (*1*−*4*), the very low-density lipoprotein (VLDL) receptor (*5, 6*), apolipoprotein E receptor 2 (apoER2) (*7*), LDL receptor-related protein (LRP1, α2-macroglobulin receptor) (*8*), LRP2 (gp330, megalin) (*9, 10*), LRP3 (*11*), LRP5 (LRP7, LR3) (*12*−*14*), LRP6 (*15*), and LR11/SorLA (*16, 17*). Human ST7, which is similar to LRP3 (*18*), *Drosophila* Yl (*19*), and the nematode *Caenorhabditis elegans* LRP are also included in this family (*20*).

The LDLR family members are typically type I membrane proteins containing a single transmembrane domain with the exception of LRP4 [which is classified as a type II membrane protein (*21*)]. In addition, they have multiple copies of a highly conserved LDLR ligand-binding repeat (LBR, class A repeat, or complement-type cysteine-rich repeat) in the extracellular region (*22*). Most members of the family also share several structural features such as: (a) epidermal growth factor (EGF)-precursor homology domains, which themselves are composed of EGF repeats (cysteine-rich class B repeats) and spacer domains with YWTD repeats, and mediate the acid-dependent dissociation of the ligands from the LDL receptor (*23*); (b) an *O*-linked sugar domain; and

[†] This work was supported in part by grants from the Ministry of Education, Science, Sports, and Culture, and by grants from the Ministry of Health and Welfare of Japan. The Department of Hematopoietic Factors is supported in part by the Chugai Pharmaceutical Co., Ltd.

[‡] The nucleotide sequence reported in this paper has been deposited in the DNA Data Bank of Japan database under DDBJ/EMBL/GenBank accession number AB042200.

* To whom correspondence should be addressed at the Department of Hematopoietic Factors, The Institute of Medical Science, University of Tokyo, 4-6-1 Shirokanedai, Minato-ku, Tokyo 108-8639, Japan. Tel: 81-3-5449-5758; Fax: 81-3-5449-5453; Email: kitamura@ims.u-tokyo.ac.jp.

[§] The Institute of Medical Science, University of Tokyo.

[||] Graduate School of Medicine, University of Tokyo.

[⊥] Takada Research Labs, Chugai Pharmaceutical Co., Ltd.

[#] Department of Anatomy and Neurobiology, Wakayama Medical School.

[▽] Research Center for Advanced Science and Technology, University of Tokyo.

[▼] Graduate School of Medicine, Chiba University.

[1] Abbreviations: apoE, apolipoprotein E; LDL, low-density lipoprotein; β-VLDL, β-migrating very low-density lipoprotein; LDLR, LDL receptor; VLDLR, VLDL receptor; apoER2, apoE receptor 2; LRP, LDL receptor-related protein; LBR, ligand-binding repeat; FH, familial hypercholesterolemia; ACAT, acyl-CoA:cholesterol *O*-acyltransferase; SST-REX, signal sequence trap by retrovirus-mediated expression screening; PAGE, polyacrylamide gel electrophoresis; PCR, polymerase chain reaction; RH, radiation hybrid.

10.1021/bi001583s CCC: $19.00
Published on Web 12/01/2000

(c) an intracellular NPXY (or FXNPXY) sequence(s).

Mutations in the LDL receptor gene are known to result in familial hypercholesterolemia (FH), which is one of the most common single gene diseases in humans. In addition, there is growing evidence that the members of the LDLR family play critical roles not only in cholesterol homeostasis, but also in vitamin metabolism and organ development (*24*−*27*).

We have recently developed a refined signal sequence trap system based on retrovirus-mediated expression screening (SST-REX) (*28*). SST-REX detects signal sequences in cDNA fragments of secreted proteins or type I membrane proteins based on their ability to redirect a signal-sequence-deficient form of a constitutively active mutant *mpl* cytokine receptor to the cell surface, thereby permitting Ba/F3 cells to grow in the absence of interleukin-3 (IL-3). Normally, Ba/F3 cells will undergo apoptosis without IL-3 supplementation. In the present study, we describe the cloning and characterization of a novel LDL receptor-related protein (LRP9) identified from a mouse lymphocyte cDNA library using SST-REX.

EXPERIMENTAL PROCEDURES

Cells. The murine IL-3-dependent pro-B cell line Ba/F3 was cultured in RPMI1640 medium (Sigma) containing 10% fetal calf serum (FCS, Sigma) and 1 ng/mL recombinant murine IL-3 (*29*). CHO-K1 and the LDL receptor-deficient ldl-A7 cells (*30*) (kindly provided by Dr. M. Krieger, MIT) were maintained in Dulbecco's modified Eagle's medium (DMEM, 4.5 mg/mL glucose, Sigma) containing 1% MEM nonessential amino acid solution (Gibco BRL) and 5% FCS (medium A). pMKITNeo/LRP9 was constructed by inserting a 2.2 kb *Xho*I−*Xho*I fragment of LRP9 cDNA into the *Xho*I sites of pMKITNeo [a modified version of the mammalian expression vector pME18S (*31*), kindly provided by Dr. K. Maruyama]. ldl-A7 cells overexpressing either LRP9 cDNA or mock vector were established by transfection with pMKITNeo/LRP9 or vector alone using Fugene6 (Boehringer Mannheim) according to the manufacturer's protocol. After selection with 1 mg/mL G418 (Sigma), survived colonies were cloned. The expression of LRP9 was quantitated by immunoprecipitation and Western blot analysis using anti-HA antibodies as described below. The highest expressing clone (ldl-A7/LRP9) was used for the subsequent experiments. In the binding assay and cholesteryl esterification assay, cells were seeded at a concentration of 5×10^5 per dish into 60 mm culture dishes containing 3 mL of medium A. On the following day, cells were washed twice with phosphate-buffered saline and refed with medium containing 5% lipoprotein-deficient serum (LPDS). Twenty-four hours later, when the cells became confluent, the cells were harvested.

Screening of a Mouse Lymphocyte cDNA Library by Signal Sequence Trap (SST). A mouse lymphocyte-derived cDNA library was screened by SST-REX as previously described (*28*, *32*). Briefly, poly(A)+ RNA was prepared from mouse lymphocytes using the FastTrack2.0 Kit (Invitrogen). Complementary DNA (cDNA) was synthesized with random hexamers, using the SuperScript Choice System (Gibco BRL) according to the manufacturer's instructions. The synthesized cDNA was size-separated by electrophoresis on an agarose gel. Fractions greater than 500 bp were collected and inserted into *Bst*XI sites of pMX-SST using *Bst*XI adapters (Invitrogen). Retroviruses representing the cDNA library were produced using an ecotropic packaging cell line, Plat-E (*33*). Ba/F3 cells were infected and selected for growth in the absence of IL-3. Genomic DNAs extracted from factor-independent clones were subjected to PCR to recover the integrated cDNAs using vector primers. The resulting PCR fragments were sequenced and analyzed. An unknown clone was obtained (SST clone 1917) and subjected to further analysis.

Cloning of the Full-Length cDNA Encoding LRP9. A biotinylated probe of 349 bp was generated by PCR from the SST clone 1917 with oligoprimers 5′GGCACTGGTAAGGAGCGATCAACTC3′ and 5′TCGGCTGTCCCGGCCTAGAG3′ using 50 μM Biotin-21-dUTP (Clontech), 200 μM each of dATP, dGTP, and dCTP, and 10 μM dTTP. To construct an oligo-dT-primed cDNA library of mouse lymphocytes, cDNA was synthesized and inserted into the *Bst*XI sites of pME18S (*31*) using *Bst*XI adapters. The cDNA library was screened using RecA protein coated with the biotinylated linear DNA probe as previously described (*34*−*36*). Several independent clones containing an open reading frame were obtained and found to encode a protein structurally similar to the LDLR. The deduced amino acid sequence of the isolated cDNA was analyzed using Genetyx-Mac (Software Development). The secondary structure of the protein was predicted using the Chou−Fasman algorithm (*37*). For further analysis, an HA-tag sequence was added to the 3′ end of the LRP9 coding region by PCR using a high-fidelity DNA polymerase, Pyrobest (Takara, Kyoto, Japan). This was accomplished by using a forward primer containing an *Xho*I site and a reverse primer containing the coding sequence for the HA epitope tag and an *Xho*I site. The amplified sequence was confirmed by sequencing.

Northern Blot Analysis. The mouse and human multiple tissue blots were purchased from Clontech. For Northern blot analysis of mouse embryo, poly(A)+ RNA of mouse embryo was purified with the FastTrack2.0 Kit (Invitrogen). Two micrograms of poly(A)+ RNA per lane was electrophoresed on a 1% agarose with 6% formaldehyde gel and blotted to Hybond-N (Amersham) as previously described (*38*). The probe used was a 0.6 kb *Xho*I−*Pst*I fragment of LRP9 cDNA.

In Situ Hybridization. To synthesize the ^{35}S-labeled riboprobes, a 0.6 kb *Xho*I−*Pst*I fragment of LRP9 cDNA was inserted into the corresponding sites of pBluescriptIISK. Linearized DNA was transcribed using T7 and T3 polymerases. In situ hybridization was performed as previously described (*39*). Briefly, adult male C57BL/6 mice were anesthetized and fixed. Frozen sections were cut on a cryostat at 6 μm thickness. After being hybridized at 56 °C for 16 h with sense and antisense ^{35}S-labeled riboprobes, the sections were submersed in Kodak NTB-2 liquid emulsion. The dipped autoradiograms were developed 21 days later and fixed. The sections were couterstained through the emulsion with hematoxylin and examined under bright-field and dark-field microscopy.

Immunoprecipitation and Western Blot Analysis. Western blot analysis was performed essentially as previously described (*38*) with some modifications. Briefly, cells were lysed in lysis buffer (25 mM Tris-HCl, pH 7.4, 1% TX-100,

10 mM EDTA, 10 mM EGTA, 10 mM sodium orthovanadate, 10 mM sodium pyrophosphate, 10 mM sodium fluoride, 1 mM PMSF). Cell lysates were immunoprecipitated with an anti-HA monoclonal antibody, 12CA5 (1.6 μg/mL, Boehringer Mannheim). SDS−polyacrylamide gel electrophoresis was performed under reducing conditions using an 8−16% gradient gel. After transfer to a nitrocellulose membrane, blots were probed with an anti-HA polyclonal antibody (diluted 1/600; Medical & Biological Laboratories, Nagoya, Japan).

Binding Assay and Cholesteryl Esterification Assay. Rabbit β-VLDL (d < 1.006 g/mL) was prepared from 1% cholesterol-fed rabbits. Male Japanese white rabbits (Saitama Experimental Animal Supply) weighing 2.5−3.0 kg were fed a 1% cholesterol diet for 3 weeks and then fasted for 15 h. A single 50 mL unit of blood was collected in 0.1% EDTA. Fractionation was carried out as previously described (*40*). β-VLDL was labeled with ^{125}I (*41*), and binding of ^{125}I-labeled β-VLDL at 4 °C was measured as described by J. L. Goldstein et al. (*41*) Protein concentrations were determined using the DC protein assay kit (Bio-Rad). The incorporation of [^{14}C]oleate−albumin into cellular cholesteryl [^{14}C]oleate by cell monolayers was measured as previously described (*41*), with the exception that β-VLDL and recombinant human apo E3 (Cosmo Bio, Tokyo, Japan) were preincubated together for 1 h at 37 °C in 250 μL of culture medium. 25-Hydroxycholesterol stimulated cholesteryl ester formation both in ldl-A7/LRP9 and in ldl-A7 to a comparable level, indicating that acyl-coenzyme A:cholesterol *O*-acyltransferase (ACAT) is expressed equivalently in both cell lines. In all assays, the mock transfectant gave results comparable to the parental ldl-A7 cell line.

Radiation Hybrid Mapping. For human radiation hybrid mapping, a PCR was run for 35 cycles under standard conditions (http://www-shgc.stanford.edu.). An oligonucleotide primer pair was designed according to the partial sequence which corresponded to the 3′ untranslated region of the human EST clone AA040020: 5′GGGCTCTACTCATAGTGGCA3′ and 5′GCTACATTANGGGTCAACGG3′. The Stanford G3 RH panel (Research Genetics) was used as PCR templates. The result was submitted to the mapping service at the Stanford Human Genome Center. For mouse radiation hybrid mapping, PCR was run for 35 cycles under standard conditions with the modification of the annealing temperature to 68 °C. An oligonucleotide primer pair was designed according to the 3′ untranslated region of mouse LRP9 cDNA: 5′GCAGGGAGAGCATTCACTGT3′ and 5′GAGTGTCCAAGCCTGTGACC3′. The T31 panel (Research Genetics) was used as the PCR templates, and results were submitted to the mapping service at the Jackson Laboratory.

RESULTS

Deduced Amino Acid Sequence of the Primary Translation. The full-length cDNA clone of LRP9 includes a 2139 bp open reading frame with an in-frame termination codon formed 162 bp upstream of the first ATG (Figure 1). The nucleotides in positions −5, −4, and −3 are in accordance with the Kozak rule (*42*). The hydrophobicity profile of the deduced amino acid sequence reveals two hydrophobic regions: one from position −17 to −1 and one from position

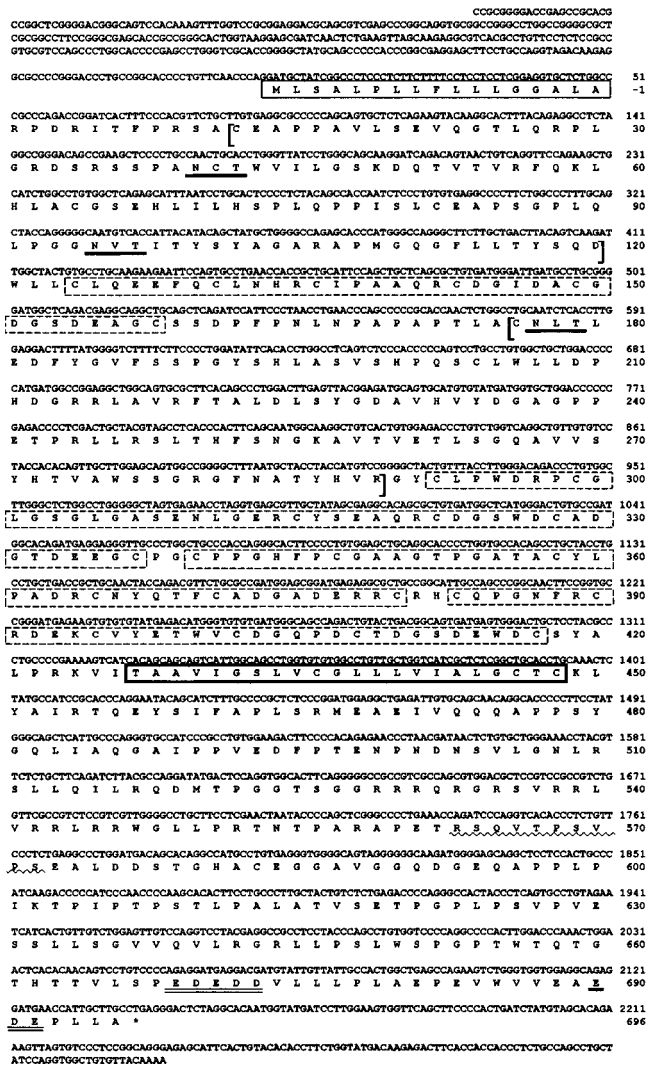

FIGURE 1: Nucleotide sequence and deduced amino acid sequence of the cDNA encoding mouse LRP9. Numbering of the amino acid sequence begins at the putative signal sequence cleavage site. The signal sequence is shown boxed with a thin line, and the transmembrane region is boxed with a thick line. The four ligand-binding repeats are boxed with broken lines. The two CUB domains are indicated with square brackets. The three potential N-glycosylation sites are underlined. The COOH-terminal acidic residues and the sequence similar to a putative basolateral sorting signal are indicated by double and wavy underlines, respectively.

+427 to +449. The former region has the characteristics of a classical signal sequence and is predicted to be posttranslationally cleaved between alanine (−1) and arginine (+1), fitting the criteria described by von Heijne (*43*). The mature protein of 696 amino acids has a calculated M_r of 74 764. The second stretch of hydrophobic residues is predicted to form a transmembrane region, suggesting that LRP9 is a type I membrane protein. Three potential N-linked glycosylation sites within the NH_2-terminal half are consistent with this view (Figure 1).

Domain Structure of Mouse LRP9 and Comparison with the Related Proteins. The NH_2-terminal 426 amino acids constitute an extracellular domain composed of 4 cysteine-rich repeats and 2 CUB domains (*44*) (Figures 1 and 3). Cysteine-rich repeats are common characteristics shared among the ligand-binding repeats (LBRs) of the LDLR family members (Figure 2A). Each LBR consists of ap-

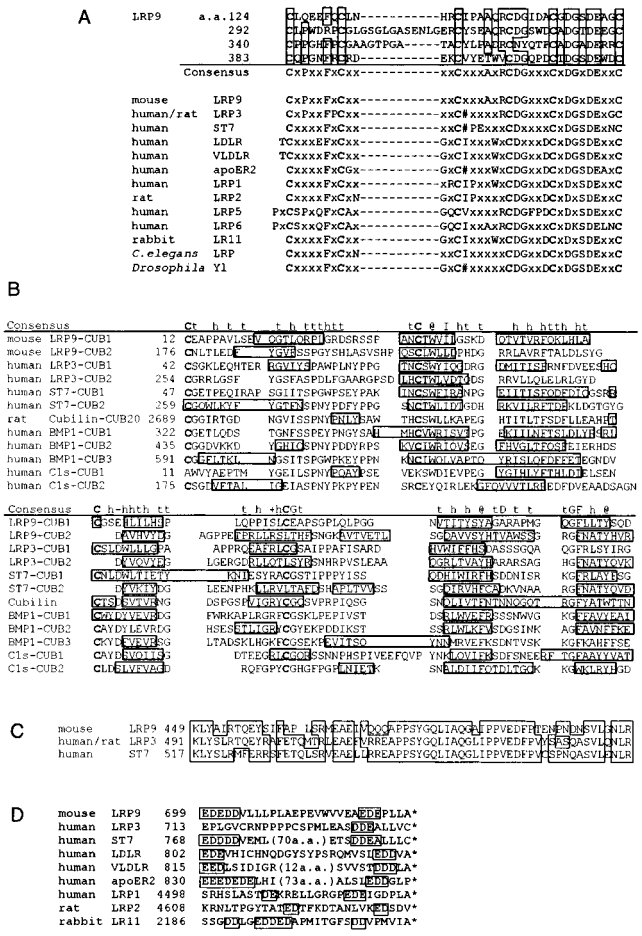

FIGURE 2: Comparison of the amino acid sequences of mouse LRP9 to related proteins. (A) The ligand-binding repeats. The conserved cysteine residues are in boldface. Amino acid residues conserved in more than 50% of the repeats are boxed and shown as a consensus sequence. Gaps are introduced so that the amino acid alignment is optimized in each repeat. #, nonpolar amino acid. (B) The CUB domains. The conserved cysteine residues are in boldface. Capitals in the consensus sequence represent strictly conserved amino acids. @, aromatic; h, hydrophobic; t, turn-like (Ser, Pro, Gly, Asp, and Asn); ±, charged amino acids. β-Strands predicted by the Chou−Fasman algorithm are boxed. (C) The juxtamembrane regions. Conserved residues are boxed. (D) The COOH-terminal residues. Conserved acidic residues are boxed. The asterisks depict stop codons. The position of the first amino acid residue of each domain is given in the third column.

proximately 40 amino acids, and approximately half of them are conserved across species ranging from *Drosophila* and *Caenorhabditis elegans* to human. In the case of the LDLR, negatively charged residues at the COOH-terminal ends of the LBRs are responsible for the binding to the corresponding positively charged sequences in apolipoprotein B-100 and apoE (*22*). The LBRs of LRP9 are also rich in acidic residues, suggesting that they are also capable of binding a specific positively charged ligand(s).

Other components found in the extracellular region are two CUB domains (Figure 2B). "CUB" is an acronym formed from complement subcomponents C1r/C1s, an embryonic sea urchin protein, Uegf, and bone morphogenic protein 1 (BMP 1) (*44*). The typical CUB domain spans approximately 110 residues and is characterized by conserved amino acid residues including 4 cysteines and by an antiparallel β-sheet structure. The physiological functions of

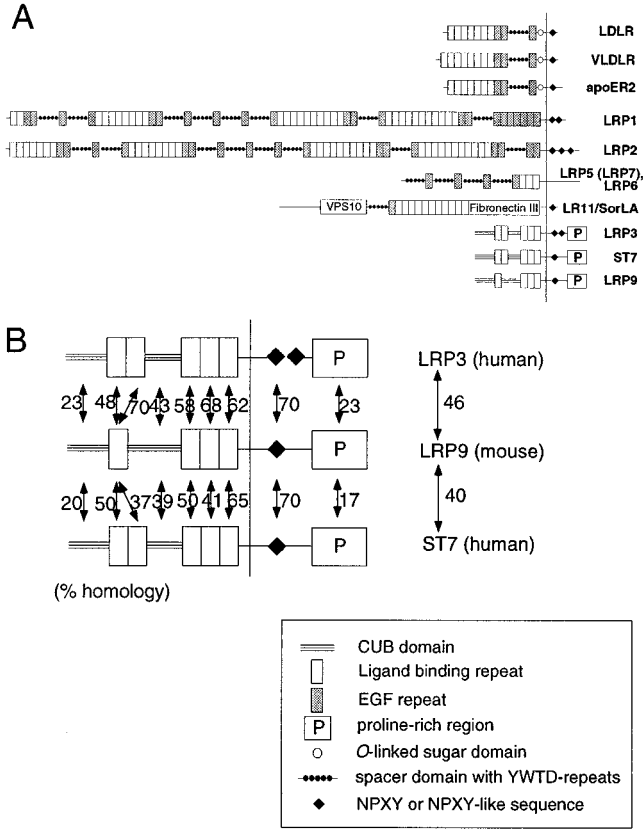

FIGURE 3: Schematic representation of LRP9 and the LDL receptor family. LRP9, LRP3, and ST7 constitute a unique subgroup of the LDLR family, characterized by the presence of CUB domains and a proline-rich region and the absence of the EGF-precursor homology domain. The homologous relationships of mouse LRP9 with human LRP3 and human ST7 are shown in panel B.

most CUB domains are unclear, but some CUB domains are reported to be involved in ligand binding (*45*−*47*). While the first CUB domain of LRP9 is typical, the second CUB domain lacks two of the four conserved cysteines as in the case of human complements C1r and C1s.

The transmembrane region is a single hydrophobic stretch of 22 amino acids immediately followed by several charged amino acids (*48*). The juxtamembrane region of LRP9 is highly homologous to those of LRP3 and ST7 (Figure 2C). An NPXY-like PPSY sequence in this region is also shared among these three related proteins. Several other characteristic features exist in the intracellular region of LRP9. The COOH-terminal 150 amino acids (Figure 1) have no homology to known proteins but are relatively proline-rich (22 proline residues in 146 amino acids). The sequence RSQVTPSVPS in positions 563−572 (Figure 1) is similar to the putative basolateral sorting signal RNxDxxS/TxxS of the LDLR and the polymeric IgA/IgM receptor (*49*). Clusters of acidic residues near the COOH-terminus (Figure 2D) are a shared feature among some members of the LDLR family (*16*). The physiological functions of these sequences are not clear.

Homology at the DNA level is 54% between LRP9 (mouse) and LRP3 (rat or human), and 49% between LRP9 and ST7 (human). The deduced amino acid sequences have 46% identity between LRP9 and LRP3 (rat or human), and 40% identity between LRP9 and ST7 (human) (Figure 3A). The entire structure of LRP9 is also similar to that of LRP3

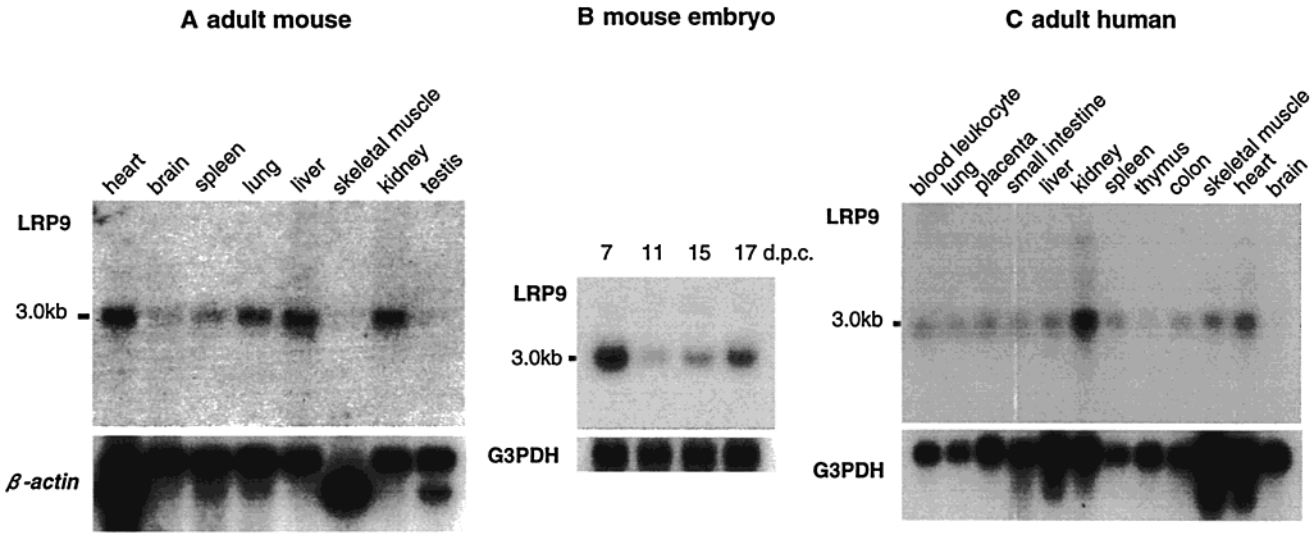

FIGURE 4: Northern blot analysis of LRP9. Poly(A)+ RNA (A, B, 2 μg/lane; C, 1 μg/lane) from the indicated tissues of adult mouse (A) or adult human (C), or from mouse embryos at the indicated stages (B) was probed with ^{32}P-labeled 0.6 kb mouse LRP9 cDNA fragment. The filters were exposed to Fuji RX-U film with an intensifying screen at −80 °C for 72 h (A, C) or 24 h (B).

with the exception of the number of the ligand-binding repeats (Figure 3A). The homology of each domain of LRP9 to the corresponding domain of LRP3 and ST7 is shown in Figure 3B.

Tissue-Specific Expression. Northern blot analysis of adult mouse tissues (Figure 4A) revealed that the 3 kb LRP9 mRNA was expressed in the heart, lung, liver, and kidney at high levels and in the brain and spleen at low levels. The expression in skeletal muscle and testis was below the detectable level. Mouse embryo also expresses LRP9 mRNA (Figure 4B). The highest expression level was obtained at 7 dpc, after which it decreased at 11 dpc and then gradually increased again. BLAST search detected a blastocyst EST clone (AA473388) identical to the partial sequence of LRP9. Northern blot analysis of adult human tissues with the mouse LRP9 probe revealed somewhat different expression patterns from adult mouse which suggests that LRP9 may play different roles in different species (Figure 4C). LRP9 mRNA was expressed rather ubiquitously in human: a transcript with a length of 3 kb was detected in blood leukocyte, lung, placenta, small intestine, liver, kidney, spleen, thymus, colon, skeletal muscle, and heart. It was below the detectable level in brain.

In Situ Hybridization Analysis. To determine what kind of cells express LRP9 in each tissue, we performed in situ hybridization in the liver, kidney, adrenal gland, and brain, areas where members of the LDLR family have been shown to play important roles (*24*−*26*) (Figure 5). In liver, LRP9 expression was detected in hepatocytes and at even higher levels in the cells of the sinusoidal lining. The transcripts in kidney were restricted to the endothelia of the peritubular capillaries. This is in contrast to LRP2/megalin which is expressed in the renal tubules (*50*) and to LRP1 which is expressed in mesangial cells (*50*). In the adrenal glands, the signals were stronger in the cortex than in the medulla. LRP9 mRNA in brain was expressed specifically in the epithelium of the choroid plexus, ependymal cells of the third ventricle, pia matter, and, to a lesser extent, hippocampal fields CA2 and CA3.

Western Blot Analysis. To estimate binding and internalization of apoE-containing lipoproteins by LRP9, the LDLR-deficient CHO-K1 cell line ldl-A7 was stably transfected with the mammalian expression vector pMKITNeo carrying LRP9 cDNA with an HA-tag at its COOH-terminus. The cell lysate of the established clone (ldl-A7/LRP9) was immunoprecipitated using an anti-HA monoclonal antibody and subjected to Western blot analysis with an anti-HA polyclonal antibody (Figure 6A). A specific 100 kDa band was detected, which is larger than the calculated molecular mass. This discrepancy in size may be explained by posttranslational glycosylation.

Cellular Uptake of β-VLDL. Next we examined whether LRP9 is capable of binding apoE-containing lipoproteins. For this purpose, β-VLDL has been often used as a ligand (*5*, *7*, *16*, *51*, *52*). β-VLDL is an apoE-rich lipoprotein detected in peripheral plasma of patients with Type III hyperlipidemia and in animals fed with a cholesterol-supplemented diet. β-VLDL is a mixture of cholesteryl ester-rich chylomicron remnants and cholesteryl ester-rich lipoproteins of liver origin (*53*).

As shown in Figure 6B, ldl-A7/LRP9 cells bound β-VLDL at concentrations of 20−50 μg of protein/mL at 4 °C. However, the binding of β-VLDL was not saturated at the ligand concentration of 50 μg of protein/mL. From the result of this rather insensitive assay (*51*), we could not conclude whether LRP9 can bind β-VLDL specifically or not (see Discussion). To verify the binding and internalization of β-VLDL, we next measured the ability of β-VLDL to stimulate the incorporation of [^{14}C]oleate into cholesteryl esters (*41*). Intracellular cholesteryl esterification is catalyzed by acyl-coenzyme A:cholesterol *O*-acyltransferase (ACAT). Cellular cholesterol synthesis itself does not stimulate ACAT activity, but rather ACAT is activated by cholesterol liberated from LDL or β-VLDL following receptor-mediated uptake (*41*). This assay is known to be much more sensitive with higher specificity than the surface binding assay using an ^{125}I-labeled ligand (*51*). As shown in Figure 7, when β-VLDL was preincubated with increasing amounts of apoE, cholesterol ester formation in ldl-A7/LRP9 cells was upregulated in a dose-dependent manner. The dose−response curve as a function of β-VLDL showed saturation kinetics. This finding is consistent with a limited number of specific surface binding sites, providing evidence that LRP9 mediates the

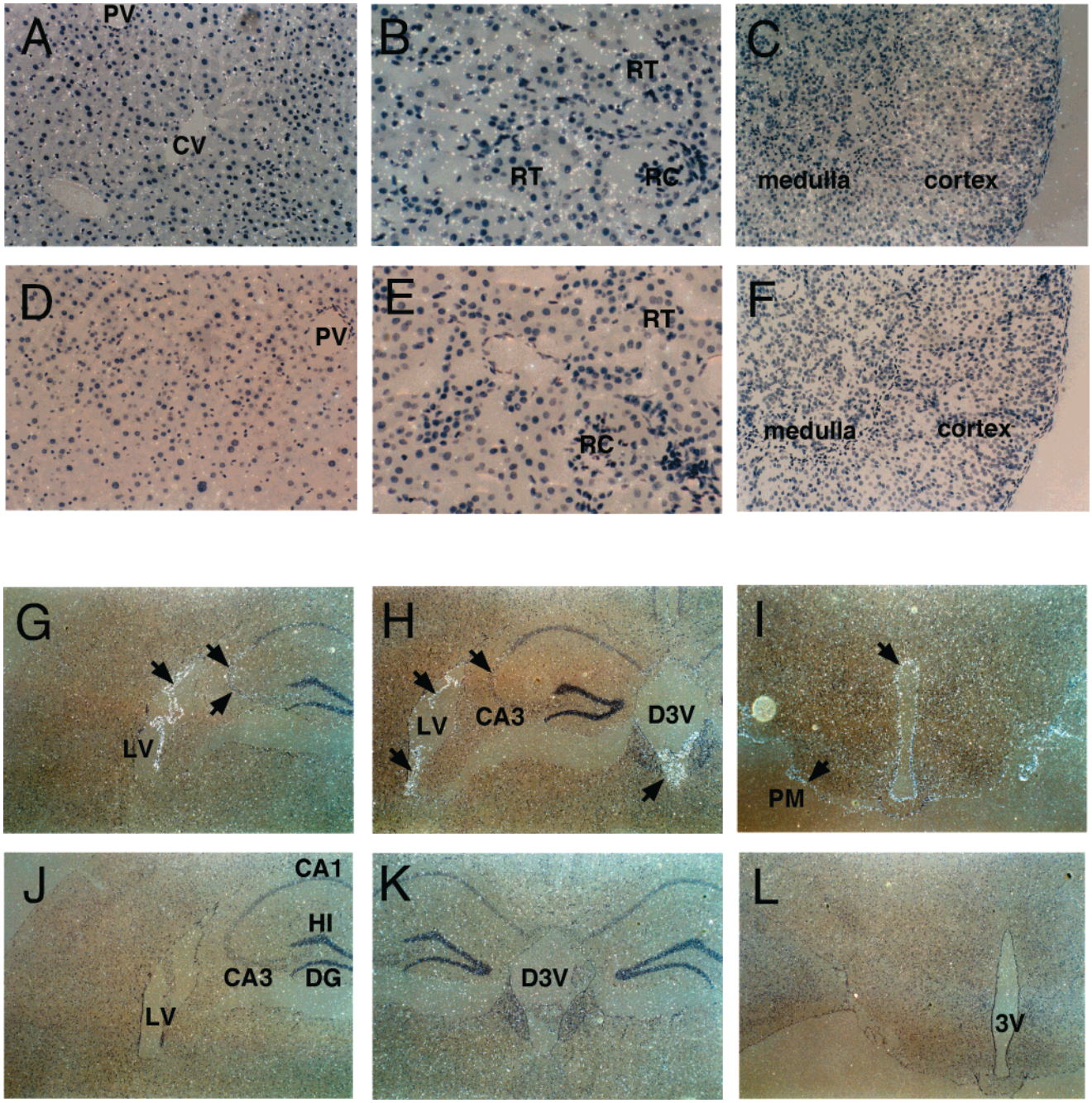

FIGURE 5: In situ hybridization of mouse liver, kidney, adrenal glands, and brain. Sections of adult mouse liver (A and D), kidney (B and E), adrenal glands (C and F), and brain (G−L) were hybridized with LRP9 antisense (A−C and G−I) or sense control (D−F and J−L) riboprobes and counterstained through emulsion with hematoxylin. Arrows indicate the signals of the choroid plexus, ependyma of the third ventricle, hippocampal fields CA2 and CA3, and pia matter. CV, central vein; PV, branch of the portal vein; RC, renal corpuscle; RT, renal tubules; HI, hippocampus; DG, dentate gyrus; 3V, third ventricle; D3V, dorsal third ventricle; LV, lateral ventricle; PM, pia matter.

uptake of apoE-enriched β-VLDL in vitro. Neither LDL (which contains apoB-100), HDL (which contains apoA-I and apoA-II), nor acetyl-LDL was capable of stimulating cholesterol ester formation in ldl-A7/LRP9 cells (data not shown).

Chromosomal Mapping. The mouse *lrp9* gene was mapped close to the markers D14Mit142, D14Mit259, and D14Mit260 on chromosome 14 using radiation hybrid (RH) mapping (Figure 8A). Human EST clones AW408759, AW410963, N47448, AA536207, and AA040020 collectively constitute a single fragment of 1565 bases and are 86% identical to the corresponding cDNA sequence of mouse LRP9. The AA040020 clone contains the sequence corresponding to the 3′ untranslated region. A primer pair was designed based on this sequence, and radiation hybrid mapping was performed. The human *lrp9* gene was mapped close to the markers SHGC-5794, SHGC-20845, and SHGC-11082 on chromosome 14q11.2 (Figure 8B). The homologous relationship between these two chromosome regions of the mouse and human is supported by the finding that human and mouse genes for T cell receptor alpha polypeptide are located very close to both of these sites.

DISCUSSION

In this paper, we have described the isolation and characterization of LRP9, a novel member of the LDLR

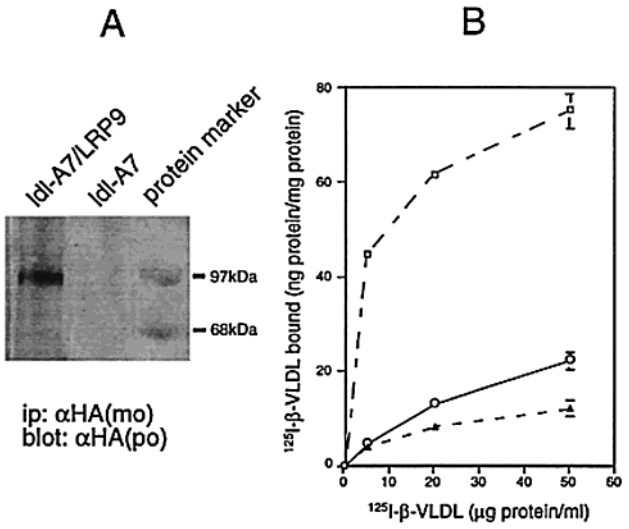

FIGURE 6: (A) Western blot analysis of the LDL receptor-deficient ldl-A7 with and without stably transfected LRP9 cDNA. Cell lysates were prepared as described under Experimental Procedures, immunoprecipitated with an anti-HA monoclonal antibody, and electrophoresed on an 8−16% gradient gel. The membrane was blotted with an anti-HA polyclonal antibody. (B) Surface binding of ^{125}I-labeled β-VLDL to monolayers of ldl-A7/LRP9 (○), ldl-A7 (△), and CHO-K1 (□) cells at 4 °C. After 24 h of growth in medium containing lipoprotein-deficient serum, cell monolayers were incubated with the indicated concentration of ^{125}I-labeled β-VLDL (412 cpm/ng of protein). After incubation for 2 h at 4 °C, the cells were washed 6 times. The amounts of surface-bound ^{125}I-labeled β-VLDL were determined as dextran sulfate-releasable fractions. The values presented are the differences between determinations made in the absence and presence of excess unlabeled β-VLDL, representing specific and high-affinity values. Each value is the average of triplicate incubations. Error bars indicate the standard deviation.

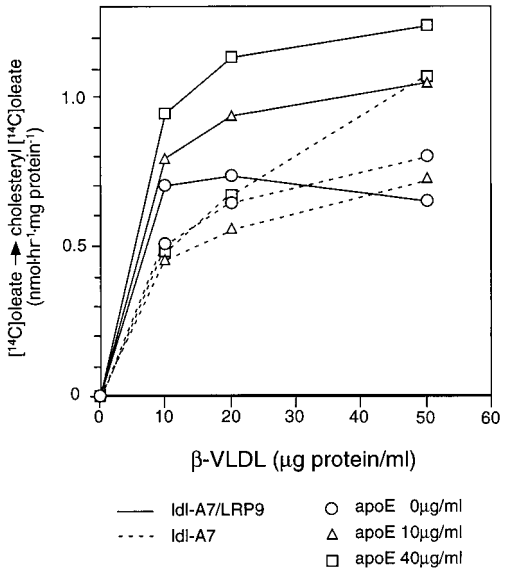

FIGURE 7: Stimulation of cholesteryl [^{14}C]oleate formation in ldl-A7/LRP9 and ldl-A7 cells by apoE-enriched β-VLDL. After 24 h of growth in medium containing lipoprotein-deficient serum, cell monolayers were incubated with the indicated concentration of β-VLDL preincubated with 0 (○), 10 (△), and 40 (□) μg/mL apoE. After 5 h, the cells were pulse-labeled for 2 h with [^{14}C]oleate, and the content of cholesteryl [^{14}C]oleate was determined. Each value is the average of duplicate incubations, which were corrected for radioactivity observed in incubations containing no lipoproteins [0.65, 0.68, and 0.70 nmol·h^{-1}·(mg of protein)$^{-1}$ for ldl-A7 with 0, 10, and 40 μg/mL apoE, respectively; 0.97, 0.96, and 0.99 nmol·h^{-1}·(mg of protein)$^{-1}$ for ldl-A7/LRP9 with 0, 10, and 40 μg/mL apoE, respectively]. ldl-A7/LRP9, solid line; ldl-A7, broken line.

family. Several unique structural features distinguish LRP9 from the two representative subgroups of this family (with the LDLR, the VLDLR, and apoER2 comprising one subgroup and LRP1 and LRP2 comprising the other): (1) a relatively small number of LBRs, (2) the presence of CUB domains, (3) the presence of a proline-rich region, (4) the absence of EGF precursor homology domains and of an *O*-linked sugar domain, and (5) a relatively large intracellular region. The previously reported proteins LRP3 and ST7 also share these features with LRP9, suggesting that they may constitute a unique subgroup of their own within the LDLR family. However, the tissue distribution of LRP9 differs from that of LRP3 (*11*) and ST7 (*18*). Human LRP3 and ST7 transcripts are expressed abundantly in brain, but their mRNA is barely detectable in liver and kidney. Thus, we expect that LRP9, LRP3, and ST7 may play different roles in vivo. The physiological importance of LRP9 is suggested by (1) the existence of two structurally related molecules which may function differently, (2) a corresponding EST clone expressed in the blastocyst stage, and (3) the highly conserved sequence alignment between mouse LRP9 and human EST clones.

It is intriguing that LRP9 is expressed in hepatocytes (Figure 4A), and that ldl-A7 cells expressing LRP9 internalized and hydrolyzed cholesterol esters in apoE-enriched β-VLDL (Figure 7). LRP1 has also been previously reported to mediate internalization and hydrolysis of cholesterol esters in β-VLDL following preincubation with apoE (*51*). However, binding of β-VLDL to LRP1 could not be detected in surface binding assays (*51*), similar to the case of LRP9 in this study. Liver-specific disruption of LRP1 in LDL receptor-deficient mice resulted in accumulation of cholesterol-rich remnant lipoproteins in the circulation, indicating a physiological role for mouse LRP1 in the uptake of remnant lipoproteins in the liver (*54*). It is believed that in vivo, apoE-rich lipoproteins similar to apoE-enriched β-VLDL are normally formed in the physiologic microenvironment prior to uptake by hepatocytes (*55*). Thus, the present study raises the possibility that LRP9 may function in an analogous fashion, as a novel receptor for apoE-containing lipoproteins. The observation that LRP9 transcripts are expressed in hepatocytes and the adrenal cortex supports this hypothesis. Although LRP9 has a relatively small number of LBRs (four LBRs), it was previously demonstrated that three LBRs in an alternatively spliced form of apoER2 were sufficient to bind β-VLDL with the same affinity as its normal form (*56*).

Alternatively, it is also possible that LRP9 may have another physiological ligand(s) in vivo other than apoE-containing lipoproteins. Some LDL receptor family members, such as VLDLR, apoER2, and LRP2, have been shown to bind apoE-containing lipoproteins in vitro (*5*, *7*, *52*). However, elevated plasma concentrations of apoE-containing lipoproteins have not been reported in mice deficient in these genes. More conclusive evidence for LRP9 function will require the generation and analysis of mice lacking LRP9.

What will be the biological role of LRP9 in the brain? The expression of LRP9 in brain was observed to be most abundant in the epithelium of the choroid plexus and the ependyma of the third ventricle (Figure 5). This may correlate

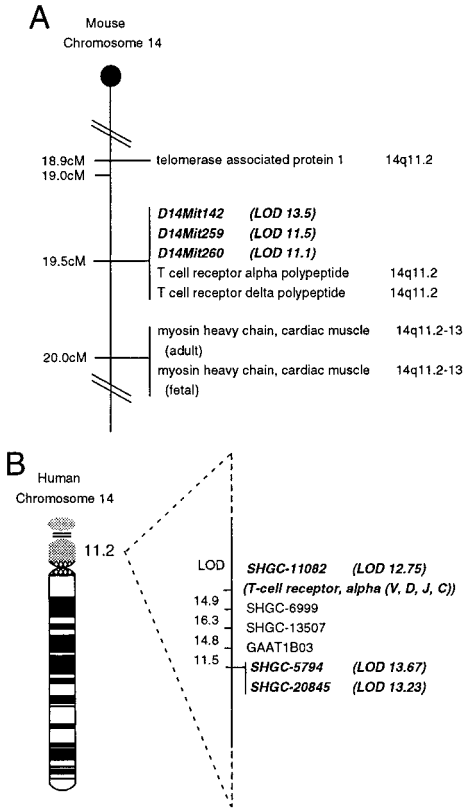

FIGURE 8: Mapping of the mouse and human *lrp9* genes. (A) The mouse *lrp9* gene was assigned to chromosome 14 by radiation hybrid (RH) mapping with LODs of 13.5 to D14Mit142, 11.5 to D14Mit259, and 11.1 to D14Mit260. Data on marker and gene positions were obtained from the Jackson Laboratory. Numbers on the left denote cM positions. The positions of loci in human chromosomes (where known) are shown to the right. (B) Human *lrp9* gene was mapped on 14q11.2 by RH mapping with LODs of 13.67 to SHGC-5794, 13.23 to SHGC-20845, and 12.75 to SHGC-11082 [T cell receptor, alpha (V, D, J, C)]. Data on marker and gene positions were obtained from the Stanford Human Genome Center (SHGC).

with the presence of apoE-containing lipoproteins in cerebrospinal fluid (*57*−*61*). Interestingly, the localization of LRP9 in mouse brain is relatively close to that of LRP2/megalin. LRP2/megalin transcripts have been detected by immunohistochemistry in ependymal cells of adult rat (*50*) and embryonic mouse (*62*) and in the choroid plexus of mouse embryo (*62*). Mice lacking LRP2/megalin display holoprosencephalic syndrome which is characterized by a lack of olfactory bulbs, forebrain fusion, and a common ventricular system (*24*). The molecular mechanism responsible for this phenotype is currently not known.

Another interesting observation is the widespread distribution of LRP9 in the vascular tissues. In particular, LRP9 is highly expressed in the peritubular capillaries of the kidney. This expression pattern is unique among the members of the LDLR family, suggesting a specific biological function of LRP9 in the kidney.

Two human heritable diseases with unknown origins, spastic paraplegia and a subtype of distal myopathies, were mapped close to 14q11.2, the same locus to which human LRP9 has also been mapped. A subtype of distal myopathies was reported to be weakly associated with MYH7 at 14q12 (*63*). Pure autosomal dominant spastic paraplegia in a family in Northern Tibet was mapped to 14q11.2-q24.3 (*64*). The association of LRP9 with these two diseases remains to be determined.

In summary, we cloned a new LDL receptor-related protein, LRP9. The protein was capable of mediating the cellular uptake and lysosomal hydrolysis of cholesterol esters in apoE-enriched β-VLDL in vitro. Further investigation is needed to clarify the biological functions of this molecule.

ACKNOWLEDGMENT

We thank Dr. M. Krieger for providing ldl-A7, Dr. K. Maruyama for pMKITNeo, A. Izumi and M. Kobayashi for excellent help in experiments, M. Ohara for language assistance, Drs. H. Shimano, T. Hamakubo, Y. Ikegaya, and Y. Sasai for invaluable discussion, and Drs. H. Bujo, K. Tsukamoto, and H. H. Cheng for critically reading the manuscript.

REFERENCES

1. Schneider, W. J., Beisiegel, U., Goldstein, J. L., and Brown, M. S. (1982) *J. Biol. Chem. 257*, 2664−2673.
2. Russell, D. W., Yamamoto, T., Schneider, W. J., Slaughter, C. J., Brown, M. S., and Goldstein, J. L. (1983) *Proc. Natl. Acad. Sci. U.S.A. 80*, 7501−7505.
3. Russell, D. W., Schneider, W. J., Yamamoto, T., Luskey, K. L., Brown, M. S., and Goldstein, J. L. (1984) *Cell 37*, 577−585.
4. Yamamoto, T., Davis, C. G., Brown, M. S., Schneider, W. J., Casey, M. L., Goldstein, J. L., and Russell, D. W. (1984) *Cell 39*, 27−38.
5. Takahashi, S., Kawarabayasi, Y., Nakai, T., Sakai, J., and Yamamoto, T. (1992) *Proc. Natl. Acad. Sci. U.S.A. 89*, 9252−9256.
6. Bujo, H., Hermann, M., Kaderli, M. O., Jacobsen, L., Sugawara, S., Nimpf, J., Yamamoto, T., and Schneider, W. J. (1994) *EMBO J. 13*, 5165−5175.
7. Kim, D. H., Iijima, H., Goto, K., Sakai, J., Ishii, H., Kim, H. J., Suzuki, H., Kondo, H., Saeki, S., and Yamamoto, T. (1996) *J. Biol. Chem. 271*, 8373−8380.
8. Herz, J., Hamann, U., Rogne, S., Myklebost, O., Gausepohl, H., and Stanley, K. K. (1988) *EMBO J. 7*, 4119−4127.
9. Raychowdhury, R., Niles, J. L., McCluskey, R. T., and Smith, J. A. (1989) *Science 244*, 1163−1165.
10. Saito, A., Pietromonaco, S., Loo, A. K., and Farquhar, M. G. (1994) *Proc. Natl. Acad. Sci. U.S.A. 91*, 9725−9729.
11. Ishii, H., Kim, D. H., Fujita, T., Endo, Y., Saeki, S., and Yamamoto, T. T. (1998) *Genomics 51*, 132−135.
12. Hey, P. J., Twells, R. C., Phillips, M. S., Yusuke, N., Brown, S. D., Kawaguchi, Y., Cox, R., Guochun, X., Dugan, V., Hammond, H., Metzker, M. L., Todd, J. A., and Hess, J. F. (1998) *Gene 216*, 103−111.
13. Dong, Y., Lathrop, W., Weaver, D., Qiu, Q., Cini, J., Bertolini, D., and Chen, D. (1998) *Biochem. Biophys. Res. Commun. 251*, 784−790.
14. Kim, D. H., Inagaki, Y., Suzuki, T., Ioka, R. X., Yoshioka, S. Z., Magoori, K., Kang, M. J., Cho, Y., Nakano, A. Z., Liu, Q., Fujino, T., Suzuki, H., Sasano, H., and Yamamoto, T. T. (1998) *J. Biochem. (Tokyo) 124*, 1072−1076.
15. Brown, S. D., Twells, R. C., Hey, P. J., Cox, R. D., Levy, E. R., Soderman, A. R., Metzker, M. L., Caskey, C. T., Todd, J. A., and Hess, J. F. (1998) *Biochem. Biophys. Res. Commun. 248*, 879−888.
16. Yamazaki, H., Bujo, H., Kusunoki, J., Seimiya, K., Kanaki, T., Morisaki, N., Schneider, W. J., and Saito, Y. (1996) *J. Biol. Chem. 271*, 24761−24768.
17. Jacobsen, L., Madsen, P., Moestrup, S. K., Lund, A. H., Tommerup, N., Nykjaer, A., Sottrup-Jensen, L., Gliemann, J., and Petersen, C. M. (1996) *J. Biol. Chem. 271*, 31379−31383.
18. Qing, J., Wei, D., Maher, V. M., and McCormick, J. J. (1999) *Oncogene 18*, 335−342.

19. Schonbaum, C. P., Lee, S., and Mahowald, A. P. (1995) *Proc. Natl. Acad. Sci. U.S.A. 92*, 1485−1489.
20. Yochem, J., and Greenwald, I. (1993) *Proc. Natl. Acad. Sci. U.S.A. 90*, 4572−4576.
21. Tomita, Y., Kim, D. H., Magoori, K., Fujino, T., and Yamamoto, T. T. (1998) *J. Biochem. (Tokyo) 124*, 784−789.
22. Krieger, M., and Herz, J. (1994) *Annu. Rev. Biochem. 63*, 601−637.
23. Davis, C. G., Goldstein, J. L., Sudhof, T. C., Anderson, R. G., Russell, D. W., and Brown, M. S. (1987) *Nature 326*, 760−765.
24. Willnow, T. E., Hilpert, J., Armstrong, S. A., Rohlmann, A., Hammer, R. E., Burns, D. K., and Herz, J. (1996) *Proc. Natl. Acad. Sci. U.S.A. 93*, 8460−8464.
25. Trommsdorff, M., Gotthardt, M., Hiesberger, T., Shelton, J., Stockinger, W., Nimpf, J., Hammer, R. E., Richardson, J. A., and Herz, J. (1999) *Cell 97*, 689−701.
26. Nykjaer, A., Dragun, D., Walther, D., Vorum, H., Jacobsen, C., Herz, J., Melsen, F., Christensen, E. I., and Willnow, T. E. (1999) *Cell 96*, 507−515.
27. Christensen, E. I., Moskaug, J. O., Vorum, H., Jacobsen, C., Gundersen, T. E., Nykjaer, A., Blomhoff, R., Willnow, T. E., and Moestrup, S. K. (1999) *J Am. Soc. Nephrol. 10*, 685−695.
28. Kojima, T., and Kitamura, T. (1999) *Nat. Biotechnol. 17*, 487−490.
29. Miyajima, A., Schreurs, J., Otsu, K., Kondo, A., Arai, K., and Maeda, S. (1987) *Gene 58*, 273−281.
30. Krieger, M., Martin, J., Segal, M., and Kingsley, D. (1983) *Proc. Natl. Acad. Sci. U.S.A. 80*, 5607−5611.
31. Kitamura, T., Hayashida, K., Sakamaki, K., Yokota, T., Arai, K., and Miyajima, A. (1991) *Proc. Natl. Acad. Sci. U.S.A. 88*, 5082−5086.
32. Fujio, K., Nosaka, T., Kojima, T., Kawashima, T., Yahata, T., Copeland, N. G., Gilbert, D. J., Jenkins, N. A., Yamamoto, K., Nishimura, T., and Kitamura, T. (2000) *Blood 95*, 2204−2210.
33. Morita, S., Kojima, T., and Kitamura, T. (2000) *Gene Ther. 7*, 1063−1066.
34. Honigberg, S. M., Rao, B. J., and Radding, C. M. (1986) *Proc. Natl. Acad. Sci. U.S.A. 83*, 9586−9590.
35. Rigas, B., Welcher, A. A., Ward, D. C., and Weissman, S. M. (1986) *Proc. Natl. Acad. Sci. U.S.A. 83*, 9591−9595.
36. Teintze, M., Arzimanoglou, II, Lovelace, C. I., Xu, Z. J., and Rigas, B. (1995) *Biochem. Biophys. Res. Commun. 211*, 804−811.
37. Chou, P. Y., and Fasman, G. D. (1978) *Annu. Rev. Biochem. 47*, 251−276.
38. Nosaka, T., Kawashima, T., Misawa, K., Ikuta, K., Mui, A. L., and Kitamura, T. (1999) *EMBO J. 18*, 4754−4765.
39. Kashiba, H., Fukui, H., Morikawa, Y., and Senba, E. (1999) *Brain. Res. Mol. Brain. Res. 66*, 24−34.
40. Kovanen, P. T., Brown, M. S., Basu, S. K., Bilheimer, D. W., and Goldstein, J. L. (1981) *Proc. Natl. Acad. Sci. U.S.A. 78*, 1396−1400.
41. Goldstein, J. L., Basu, S. K., and Brown, M. S. (1983) *Methods Enzymol. 98*, 241−260.
42. Kozak, M. (1987) *Nucleic Acids Res. 15*, 8125−8148.
43. von Heijne, G. (1984) *J. Mol. Biol. 173*, 243−251.
44. Bork, P., and Beckmann, G. (1993) *J. Mol. Biol. 231*, 539−545.
45. Kristiansen, M., Kozyraki, R., Jacobsen, C., Nexo, E., Verroust, P. J., and Moestrup, S. K. (1999) *J. Biol. Chem. 274*, 20540−20544.
46. Nakamura, F., Tanaka, M., Takahashi, T., Kalb, R. G., and Strittmatter, S. M. (1998) *Neuron 21*, 1093−1100.
47. Thielens, N. M., Enrie, K., Lacroix, M., Jaquinod, M., Hernandez, J. F., Esser, A. F., and Arlaud, G. J. (1999) *J. Biol. Chem. 274*, 9149−9159.
48. Sabatini, D. D., Kreibich, G., Morimoto, T., and Adesnik, M. (1982) *J. Cell Biol. 92*, 1−22.
49. Yokode, M., Pathak, R. K., Hammer, R. E., Brown, M. S., Goldstein, J. L., and Anderson, R. G. (1992) *J. Cell Biol. 117*, 39−46.
50. Zheng, G., Bachinsky, D. R., Stamenkovic, I., Strickland, D. K., Brown, D., Andres, G., and McCluskey, R. T. (1994) *J. Histochem. Cytochem. 42*, 531−542.
51. Kowal, R. C., Herz, J., Goldstein, J. L., Esser, V., and Brown, M. S. (1989) *Proc. Natl. Acad. Sci. U.S.A. 86*, 5810−5814.
52. Willnow, T. E., Goldstein, J. L., Orth, K., Brown, M. S., and Herz, J. (1992) *J. Biol. Chem. 267*, 26172−26180.
53. Fainaru, M., Mahley, R. W., Hamilton, R. L., and Innerarity, T. L. (1982) *J. Lipid Res. 23*, 702−714.
54. Rohlmann, A., Gotthardt, M., Hammer, R. E., and Herz, J. (1998) *J. Clin. Invest. 101*, 689−695.
55. Mahley, R. W., and Ji, Z. S. (1999) *J. Lipid Res. 40*, 1−16.
56. Kim, D. H., Magoori, K., Inoue, T. R., Mao, C. C., Kim, H. J., Suzuki, H., Fujita, T., Endo, Y., Saeki, S., and Yamamoto, T. T. (1997) *J. Biol. Chem. 272*, 8498−8504.
57. Yamauchi, K., Tozuka, M., Hidaka, H., Hidaka, E., Kondo, Y., and Katsuyama, T. (1999) *Clin. Chem. 45*, 1431−1438.
58. Guyton, J. R., Miller, S. E., Martin, M. E., Khan, W. A., Roses, A. D., and Strittmatter, W. J. (1998) *J. Neurochem. 70*, 1235−1240.
59. Rebeck, G. W., Alonzo, N. C., Berezovska, O., Harr, S. D., Knowles, R. B., Growdon, J. H., Hyman, B. T., and Mendez, A. J. (1998) *Exp. Neurol. 149*, 175−182.
60. Borghini, I., Barja, F., Pometta, D., and James, R. W. (1995) *Biochim. Biophys. Acta. 1255*, 192−200.
61. Pitas, R. E., Boyles, J. K., Lee, S. H., Hui, D., and Weisgraber, K. H. (1987) *J. Biol. Chem. 262*, 14352−14360.
62. Kounnas, M. Z., Haudenschild, C. C., Strickland, D. K., and Argraves, W. S. (1994) *In Vivo 8*, 343−351.
63. Laing, N. G., Laing, B. A., Meredith, C., Wilton, S. D., Robbins, P., Honeyman, K., Dorosz, S., Kozman, H., Mastaglia, F. L., and Kakulas, B. A. (1995) *Am. J. Hum. Genet. 56*, 422−427.
64. Huang, S., Zhuyu, Li, H., Labu, Baizhu, Lo, W. H., Fischer, C., and Vogel, F. (1997) *Hum. Genet. 100*, 620−623.

BI001583S